

# Control of Odors and VOC Emissions

**April 20-23, 1997**  
**Adam's Mark Hotel**  
**Houston, Texas U.S.A.**

Held in cooperation with the Water  
Environment Association of Texas.

 **Water Environment  
Federation®**  
*Preserving & Enhancing  
the Global Water Environment*

PROCEEDINGS

***Control of Odors  
and  
VOC Emissions  
Specialty Conference***

April 20-23, 1997  
Adams Mark Hotel  
Houston, Texas

**Held in Cooperation with  
the  
Water Environment  
Association of Texas**

# ANALYSIS OF FLUX CHAMBERS FOR MEASURING VOC EMISSIONS AT SOIL AND WATER SURFACE

Fang Gao, WEF Member, and S. R. Yates  
U. S. Salinity Laboratory  
U. S. Department of Agriculture  
450 West Big Springs Road, Riverside, California 925074617

## INTRODUCTION

Flux chamber methods have been used for measuring gas emissions from soil into the atmosphere. Examples include emissions from agricultural fields and waste treatment and disposal sites (Denmead, 1979; Matthias et al., 1980; Sanders et al., 1985; Balfour et al., 1987; Yagi et al., 1995; Yates et al., 1996). Applications of flux chambers for measuring gas emissions at water surface, wastewater surface and wetland surface have been also reported in the literature (e.g., Sebacher et al., 1983; Woodrow and Seiber, 1991; Gholson et al., 1991). In general, these methods involve placing an open-bottom enclosure at the soil or water surface, monitoring the target gas concentration within the enclosure during chamber placement, and estimating the emission rate (i.e., flux density) from the concentration data (Rolston, 1986). The major advantages of using flux chambers are low cost, simplicity of fabrication and installation, easy operation, and capability for measuring gas emissions from small land or water surfaces.

Although flux chambers have been widely used for many years, some problems associated with them remain unsolved. For example, a dynamic chamber is often cited to overestimate the actual fluxes due to an additional advective mass flow of the target gas induced by a pressure deficit created by flowing air through the chamber (Rolston, 1986; Wesely et al., 1989). Kanemasu et al. (1974) demonstrated that a pressure deficit as small as 1 Pa could induce significant mass flow and thus severely overestimate the emission rate. Although their work has been cited often with regard to overestimating the emission rate when using a dynamic chamber, their study should be considered as a special case because they used a large chamber with relatively small inlet and outlet and they maintained a high air flow rate of  $2.8 \text{ m}^3 \text{ min}^{-1}$  or  $2800 \text{ L min}^{-1}$ . This flow rate is not representative of the air flow rates commonly reported in the literature. However, their results demonstrate the importance of the air flow rate and inlet/outlet dimensions in controlling dynamic chamber behavior.

In a recent experiment, we studied the effects of air flow rate, soil permeability, and various soil surface conditions, on the steady-state emission rates measured by a thin, square dynamic chamber. We found from this experiment that the steady-state flux increased with the air flow rate, especially when the dynamic chamber was operating at the open surface of a coarse sand medium. We measured the pressure deficits within the chamber at various air flow rates. We noted that the pressure deficits were significantly greater than the values estimated by the velocity of the flowing air. It was suspected that the laboratory vacuum system, which was used to induce the airstream through the chamber, was contributing to the pressure deficits within the chamber. This prompted an exploration of the relationship between the pressure deficit and the airflow rate, and the chamber inlet dimensions. Another topic of interest is the leaks of the chamber body that may affect the flux measurement. The effect of the chamber leakage on the flux measurement can be caused by either the intrusion of the outside contaminated air into the chamber or the escape of the chamber air (i.e., the air inside the chamber) to the outside environment. In other words, the target gas concentration in the chamber airstream is not representative solely of the emission from the covered soil surface. In addition, the effect of chamber leakage can be also due to the pressure change within the chamber since any leaks on the chamber body will alter or relieve the pressure deficit within the chamber. Since the pressure deficit has a significant impact on the flux measurement, the influence of the chamber leaks on the pressure deficit should be also explored.

In this paper, we will present and discuss our experimental data to show how the vacuum source, the air flow rate, the chamber inlet dimensions, and the possible leaks of the chamber body affect the pressure deficit, and thus, the flux density measured by the dynamic chamber. Some implications from our laboratory experimental results, which are helpful for the proper field application of dynamic chambers, will be also discussed.

## **METHODOLOGY**

The experimental setup is shown in Figure 1. During the experiment, the experimental system was placed under a ventilated laboratory fume hood at an ambient temperature of 25°C.

### ***Soil Matrix***

The soil matrix (Figure 1a) was packed in an open-top plastic box which had a width of 30 cm, a length of 50 cm and a height of 20 cm. Two soils were used in the experiment: commercially available #60 fine sand and #12 coarse sand. The air permeabilities for the two media were estimated to be approximately  $3 \times 10^{-7}$  and  $3 \times 10^{-6} \text{ cm}^2$  for the fine sand and the coarse sand, respectively, from their saturated hydraulic conductivities measured using the falling head method (Klute and Dirksen, 1986; Massmann, 1989). Two surface conditions were studied for the soil matrix in the experiment: (1) open to the ambient air, and (2) covered with one layer of high-density polyethylene tarp (0.025mm thick) commonly used in agricultural fumigation. The reason of using this physical barrier at the soil surface was to study a system where the pressure deficit within the chamber would not be relieved by the air moving out from the covered soil matrix.

### ***Dynamic Chamber***

The structural details and aerodynamic features of the dynamic chamber used in this experiment have been reported previously (Gao et al., 1996). The chamber used in this study has a width ( $W$ ) of 20 cm, a length ( $L$ ) of 19.8 cm, and a height ( $H$ ) of 5 cm (Figure 1a). In brief, the dynamic chamber has an inlet, a wedge-shaped inlet transition zone, a square body that covers the soil surface with an area ( $A$ ) of  $396 \text{ cm}^2$  (i.e.,  $A = W \times L$ ), a wedge-shaped outlet transition zone, and an outlet. Within each transition zone, five separation baffles were installed to divide the zone into six individual channels to direct the flowing air uniformly across the entire enclosed soil surface. When operating at an open soil surface, the chamber was placed on a metal frame inserted into the soil matrix to a depth of 5 cm (Figure 1a). When operating at the tarped (i.e., covered) soil surface, the chamber was placed directly on the tarp. The airstream through the chamber was induced by a laboratory vacuum at the outlet side of the chamber. The air flow rate was regulated by a valve and monitored by a Manostat ball flow meter (Manostat Corp., New York, NY). In this study, a 0.3 cm thick transparent PVC (polyvinyl chloride) cover was installed on the chamber. The cover had thirty evenly-distributed probe holes (0.5 cm in diameter), as shown in Figure 1a, to allow measurement and sampling at specific locations within the chamber. These holes were sealed with small rubber stoppers when not in use. Four different inlets (Figure 1 b) were used in this experiment to observe the effects of inlet dimensions on the pressure deficit. With these 4 inlets, we could compare two inlets with the same opening diameter but different lengths (inlet 1 vs. inlet 2, or inlet 3 vs. inlet 4), and two inlets with the same length but different diameters (inlet 1 vs. inlet 3, or inlet 2 vs. inlet 4). Two sets of tests were conducted to measure the pressure deficits within the dynamic chamber, as described in the following section.

### ***Experimental Procedures***

In the first set of tests, the dynamic chamber was operated individually on the covered surface of fine sands, the open surface of fine sands, and the open surface of coarse sands at an air flow rate of 21 L

$\text{min}^{-1}$ . All four inlets (Figure 1 b) were tested individually in each individual test. The pressure deficits within the chamber, with respect to the ambient pressure, were measured about 3 cm above the soil surface through five randomly-selected probe holes, i.e., at five different locations within the chamber. Pressure deficit data from five locations were believed to be representative, because a preliminary test showed that the pressure deficit within the chamber had a uniform distribution at a given air flow rate. When the pressure deficit was measured through one probe hole, all other holes were kept sealed with small rubber stoppers. A low range (0 to 25 Pa) pressure transducer, Model PX653-0.1 D5V (Omega Engineering, Inc., Stamford, CT), was used to measure the pressure deficit, and a digital datalogger, Micrologger Model 21X (Campbell Scientific, Inc., Logan, UT), was used for data acquisition. The data logger read the pressure deficit every 0.5 s, averaged the readings every minute, and recorded the average. At least two averages were obtained from each of the five locations within the chamber in one individual test. To minimize the effect of the ventilation air in the fume hood on the measured pressure deficit, the open end of the high-pressure probe tubing was placed in an open 125-mL Erlenmeyer flask (Figure 1 a).

The purpose of the second set of tests was to examine the effect of the dimensions of the chamber inlet (size of opening and length) on the pressure deficit within the chamber. Two tests were conducted on the open surfaces of the fine sands at two different air flow rates, 37 and 21  $\text{L min}^{-1}$ , respectively, and one test was conducted on the open surface of the coarse sands at an air flow rate of 21  $\text{L min}^{-1}$ . In all three tests, each of the four inlets was used individually (i.e., in an individual run). During the test with each individual inlet, the 12 probe holes at the inlet side (as shaded in Figure 1a for distinction) were opened consecutively with a random sequence and the pressure deficit was measured within the chamber after each additional hole was opened. Since each probe hole had a diameter of 0.5 cm, one open hole added an approximately  $0.2 \text{ cm}^2$  opening for the chamber inlet. The procedures of pressure measurement was the same as described in the first set of tests.

## RESULTS

### **First Set of Tests**

The pressure deficits measured in the first set of tests are plotted in Figure 2. The term “pressure deficit” used here and hereafter represents the absolute value or magnitude of the difference between the pressure of the airstream within the chamber and the ambient pressure in still air (i.e., in the Erlenmeyer flask). The pressure deficits corresponding to four different inlets in three tests are placed in three individual groups for comparison purpose. The estimated pressure deficits in Figure 2 are calculated using Poiseuille’s law, assuming the air flow in the inlet pipe is laminar and incompressible (de Nevers, 1991)

$$\Delta P = \frac{40LQ\mu}{3\pi R^4} \quad (1)$$

where  $\Delta P$  is the pressure difference across the inlet pipe (Pa),  $L$  is the length of the inlet pipe (cm),  $Q$  is the air flow rate through the pipe ( $\text{L min}^{-1}$ ),  $R$  is the radius of the inlet pipe (cm), and  $\mu$  is the viscosity of the ambient air which has a value of  $1.85 \times 10^{-4} \text{ g cm}^{-1} \text{ s}^{-1}$  (Weast, 1986). Due to the configuration of our dynamic chamber, the airstream in the chamber maintains a uniform air velocity at a given flow rate (Gao et al., 1996). Thus, we can apply Bernoulli’s equation to estimate the pressure difference between the flowing airstream inside the chamber and the stagnant air phase in the soil matrix, using the air flow rate and the chamber dimensions (de Nevers, 1991)

$$\Delta P = \frac{10^{-4}}{2} \rho_{air} V_{air}^2 = \frac{\rho_{air}}{72} \left( \frac{Q}{HW} \right)^2 \quad (2)$$

where  $\rho_{air}$  is the density of ambient air that has a value of  $1.30 \text{ mg cm}^{-3}$  (Weast,1986),  $V_{air}$  is the velocity of flowing air through the chamber ( $\text{cm s}^{-1}$ ),  $H$  and  $W$  are the chamber height and width (cm), respectively. Using Eq.(2), we can obtain  $\Delta P$  values of  $2.5 \times 10^{-3}$  and  $0.8 \times 10^{-3}$  Pa for the air flow rates of  $37$  and  $21 \text{ L min}^{-1}$ , respectively. We define  $\Delta P$  calculated from Eq.(2) to be the pressure deficit caused by the flowing air within the dynamic chamber.

### **Second Set of Tests**

The pressure deficits measured in the second set of tests are shown in Figure 3 through Figure 5. The discrete number on the horizontal axis of these figures represents the number of the probe holes opened for the corresponding pressure measurement. To illustrate the magnitudes of the pressure deficits and to facilitate our discussion in the following sections, we also list in Table 1 the largest and smallest pressure deficits, which correspond to  $\Delta P_0$  (with no open probe hole) and  $\Delta P_{12}$  (with 12 open probe holes), respectively.

## **DISCUSSION**

### **First Set of Tests**

We first examine how the pressure deficits within the dynamic chamber differ when the chamber operates at different **soil** surfaces. The first set of columns in Figure 2 (labeled as CS) are the pressure deficits for the covered fine sand surface. The observed pressure deficits **for this case are higher than the pressure deficits measured at the open surface of the fine sands (labeled as OSFS), which are higher than those measured at the open surface of the coarse sands (labeled as OSCS).** The presence of the plastic tarp at the surface of the fine sands adds a physical barrier to reduce significantly the advective inter-facial air transport which would otherwise relieve the pressure deficit within the chamber. If we assume that the tarped surface to be equivalent to a soil matrix with an even lower permeability, we can see that the lower the permeability of the soil matrix, the higher the pressure deficit is within the dynamic chamber at a given air flow rate.

The last set of columns in Figure 2 is calculated for the four inlets using Eq.( 1). If we compare these estimated (or calculated) pressure deficits and those actually measured, we can see that the estimated pressure deficits are smaller than the measured values for all four inlets with all three surface conditions. The comparison indicates that under the conditions of this experiment, using Poiseuille's law and the chamber inlet dimensions and the air flow rate to calculate  $\Delta P$  will lead to underestimate of the actual pressure deficit within the chamber. This implies that the vacuum operating at the outlet side of the chamber contributes significantly to the pressure deficit inside the dynamic chamber in this experiment. From the four sets of data in Figure 2, it can be seen that the lower the permeability of the soil matrix, the greater the contribution of the operating vacuum to the pressure deficit is.

One important point in Figure 2 is the effect of the chamber inlet dimensions on the pressure deficit within the chamber. From all three sets of the measured pressure deficits, it can be seen that the inlet dimensions have a significant effect on the measured pressure deficit. The numerical values of the first set of pressure deficits in Figure 2 (CS set) are 0.15, 0.32, 3.92 and 6.82 Pa for the inlets 1, 2, 3 and 4 (Figure 1 b), respectively. The numerical values of the pressure deficits for the OSFS and OSCS sets in Figure 2 are listed in the column under  $\Delta P_0$  with the air flow rate of  $21 \text{ L min}^{-1}$  in Table 1. The inlets 1

and 2 have the same cross-section area ( $12.57 \text{ cm}^2$ ), and the inlet 3 and 4 have the same cross-section area ( $2.01 \text{ cm}^2$ ). The inlet 2 and 4 are approximately 5 times longer than the inlets 1 and 3. On the other hand, the cross-section area of the inlets 1 and 2 is approximately 6 times larger than that of the inlets 3 and 4. Comparison of these three sets of pressure deficits can lead to some meaningful information. First, when the inlet cross-section area is the same (e.g., inlets 1 and 2, or inlets 3 and 4) the longer the inlet pipe, the greater the pressure deficit is within the chamber. In this experiment, however, the longer inlets (2 and 4) resulted in the pressure deficits only about twice as large as the shorter inlets (1 and 3). Second, when the length of the inlet pipe is the same (e.g., inlets 1 and 3, or inlets 2 and 4), the smaller the cross-section of the pipe, the greater the pressure deficit is inside the chamber. In this experiment, the smaller inlet pipes (3 and 4), which were about 6 times smaller in cross-section area, lead to the pressure deficits about 15 to 25 times larger than those caused by the larger inlet pipes (1 and 2). It is clear that the cross-section area (i.e., the opening area) of the chamber inlet plays a more important role than the length of the inlet pipe in controlling the pressure deficit within the chamber. It is worthwhile to note that Poiseuille's law produces very similar estimates in terms of relative importance of the chamber inlet dimensions for the pressure deficits within the chamber.

It should be noted also that the pressure deficits measured in all three tests are much larger, at least two orders of magnitude larger, than the values estimated by Eq.(2). As mentioned earlier, the measured pressure deficits are also significantly greater than the values calculated using Eq.(1), especially when the chamber is operating at the covered soil surface and on the fine sands (less permeable as compared to the coarse sands). This indicates that for the vacuum-operated chamber system tested in this experiment the pressure deficit within the chamber is primarily created by the operating vacuum, and the pressure deficit caused by the flowing air can be neglected.

### **Second Set of Tests**

The pressure deficits measured within the dynamic chamber in the second set of tests show a similar trend as shown in the first set of tests, i.e., decreasing when the number of the open probe holes was increasing (Figures 3, 4 and 5). From each of Figures 3, 4 and 5, it can be seen clearly that when the initial inlet opening is smaller (i.e., inlets 3 and 4), addition of one open hole has a much greater impact on the pressure deficit within the chamber. The decreasing rates of the pressure deficit in the chamber with inlets 3 and 4 are significantly greater than those with inlets 1 and 2. This is especially obvious when we look at the decreasing trends along with the first several open probe holes. This can be explained by the relative sizes of the inlet opening and the probe hole opening. Each probe hole has an opening of  $0.2 \text{ cm}^2$ , approximately 10% of the cross-section area of the inlets 3 and 4 ( $2.01 \text{ cm}^2$ ), but only 1.6% of the inlets 1 and 2 ( $12.57 \text{ cm}^2$ ). When all 12 probe holes are open, the total additional opening is  $2.4 \text{ cm}^2$ , which is 119.4% of the opening of the inlets 3 and 4, but only 19.1% of the inlets 1 and 2. Experimental data and calculations in Table 1 show that when all 12 probe holes are open, the pressure deficits within the chamber ( $\Delta P_{12}$ ) dropped by about 90% from their initial values ( $\Delta P_0$ ) when using the inlets 3 and 4, while by about 40% from their initial values when using the inlets 1 and 2.

All three figures and data in Table 1 show that when the inlet opening is the same (inlets 1 and 2, or inlets 3 and 4), the length of the inlet pipe also has an effect on the changing behavior of the pressure deficit while the additional probe holes were opened. The longer the inlet pipe, the faster the pressure deficit decreased while additional probe holes were opened. With a length difference of 5 times (22 cm for inlet 1 versus 102 cm for inlet 2, and 22 cm for inlet 3 versus 102 cm for inlet 4). the differences in the ratios of  $\Delta P_{12} / \Delta P_0$  are several percent for all tests, as indicated in Table 1. However, the magnitude of decrease of pressure deficits for the first couple of open holes are significant for the small inlets. For example, the differences of  $\Delta P_0 - \Delta P_1$  ( $\Delta P_1$  is the pressure deficit measured with one open probe hole) are 0.72 and 1.75 Pa for inlets 3 and 4, respectively, while the differences of  $\Delta P_0 - \Delta P_1$  for inlets 1 and 2 are only 0.01 and 0.03 Pa, respectively.

Comparison of Figures 3 and 4 shows how the number of open probe holes affects the measured pressure deficit when the chamber was operating at the open surface of fine sands at two different flow rates, i.e., 37 and 21 L min<sup>-1</sup>. At a higher air flow rate the pressure deficit within the chamber decreases with greater magnitudes as the number of open probe holes increases. This can be seen if we compare the results in the column under  $\Delta P_0 - \Delta P_{12}$  in Table 1. Also, the differences of  $\Delta P_0 - \Delta P_1$  at an air flow rate of 37 L min<sup>-1</sup> are 1.16 and 2.86 Pa for inlets 3 and 4, respectively, and greater than those at an air flow rate of 21 L min<sup>-1</sup> (0.72 and 1.75 Pa).

We can also compare Figure 4 and 5, the change of the measured pressure deficit when the chamber was operating on two different soils (fine sand and coarse sand) at a same air flow rate of 21 L min<sup>-1</sup>. It can be seen that the effect of increasing the number of open probe holes on the resulting pressure deficit is greater when the chamber is operating on the fine sand (less permeable) than on the coarse sand (more permeable). The differences of  $\Delta P_0 - \Delta P_1$  on the fine sands are 0.72 and 1.75 Pa for inlets 3 and 4, respectively, which are greater than those on the coarse sands, 0.41 and 0.74 Pa for inlets 3 and 4, respectively.

One implication of the above discussion for the practical chamber application is the effect of possible leaking of dynamic chambers during operation. If a dynamic chamber has leaks during its operation, the pressure deficit inside the chamber will be affected by those leaks. Thus, the gas flux at the soil surface will be affected as well, since the pressure deficit has a significant impact on the gas flux at the soil surface (Kanemasu et al., 1974; Rolston, 1986). The effect of leaking will be especially severe when the chamber inlet is relatively small and a long inlet pipe is attached. The pressure deficit data in all three tests (Figures 3, 4 and 5) show that the addition of a small open hole, which can be treated as an artificial leak, to the inlets 3 and 4 can drastically change the pressure deficit within the chamber. This implies that if two same chambers are operating in the field under the same conditions but one (or both) of them is not properly sealed, the two chambers may produce different flux measurements even though the emission rates at the two chamber locations may be the same. This may be one reason why the flux measurements by the chamber methods are likely variable in the field application. The leakage factor (i.e., the degree of leaking) of each chamber, or the same chamber at different locations, is likely highly variable. Further, if a dynamic chamber has leaks, air outside the chamber will be sucked into the chamber through these leaks. In general, the air around the chamber contains the target gas and the intrusion of such air into the chamber will add an extra mass of the target gas to the main airstream in the chamber. Since this extra mass could not be measured, the leaks would lead to errors in the flux measurements. Two possible causes for chamber leakage include deformation of chamber body during shipment, installation and ambient temperature change, and improper connection between chamber components, such as between chamber body and chamber base frame. Thus, great care must be taken in fabrication, shipment, installation, and operation of dynamic chambers to avoid any possible leaks.

## CONCLUSIONS

The purpose of this study is to identify the major cause of the pressure deficit within the dynamic chamber, and to obtain information on the relationship between the pressure deficit and the chamber inlet dimensions and the air flow rate. The following conclusions can be drawn from the results obtained from this study.

- (1) For our vacuum-operated dynamic chamber, the pressure deficit within the chamber is caused primarily by the operating vacuum, rather than by flowing air. Using Poiseuille's law and chamber inlet dimensions to calculate the pressure deficit will lead to underestimate of the actual pressure deficit.
- (2) Dimension of the chamber inlet has a significant effect on the pressure deficit. Increasing the size

of inlet opening can significantly reduce the magnitude of pressure deficit within the dynamic chamber, It is suggested that large openings for chamber inlets be selected when designing and fabricating dynamic chambers. If the inlet opening is large enough, the pressure deficit created by the operating vacuum may be controlled within a certain range, thus limiting its effect on flux measurement.

(3) The air flow rate under vacuum also affects the pressure deficit within the dynamic chamber. The higher the air flow rate, the greater the pressure deficit is inside the chamber during operation. This reflects indirectly the cause-and-effect relationship between the vacuum and the pressure deficit, since the higher air flow rate is driven by a stronger vacuum (i.e., negative pressure),

(4) Leaking of the chamber system during operation will cause significant difference in the pressure deficits, especially for a dynamic chamber with a small inlet opening. This may be a possible factor causing variation of flux measurements in the field. Our experimental data indicates that sealing the chamber to avoid leakage is extremely important for maintaining proper chamber operation. Thus, all necessary measures need to be taken to eliminate possible leaks when using dynamic chambers.

#### ACKNOWLEDGMENT

The authors thank Dr. D. Wang and Ms. Q. Zhang for their help in part of the experiment reported in this paper.

#### REFERENCES

Balfour, W. D., Schmit, C. E., and Eklund, B. M., (1987) Sampling approaches for the measurement of volatile compounds at hazardous waste sites. *J. Hazard. Mat.*, 14, 135-148.

de Nevers, N., (1991) Fluid mechanics for chemical engineers. 2nd ed. McGraw-Hill, *Inc.*, New York, NY.

Denmead, O. T., (1979) Chamber systems for measuring nitrous oxide emission from soils in the field. *Soil Sci. Soc. Am. J.*, 43, 89-95.

Gao, F., Yates, S. R., M. V. Yates, Gan, J., and Ernst, F. F., (1996) Design, fabrication, and application of a dynamic chamber for measuring gas emissions from soil. *Environ. Sci. Technol.* (in press).

Gholson, A. R., Albritton, J. R., Jayanty, R. K. M., Knoll, J. E., and Midgett, M. R., (1991) Evaluation of an enclosure method for measuring emissions of volatile organic compounds from quiescent liquid surface. *Environ. Sci. Technol.*, 25, 519-524.

Kanemasu, E. T., Powers, W. L., and J. W. Sij, (1974) Field chamber measurements of CO<sub>2</sub> flux from soil surface. *Soil Sci.*, 118, 233-237.

Matthias, A.D., Blackmer, A. M., and Bremner, J. M., (1980) A simple chamber technique for field measurement of emissions of nitrous oxide from soils. *J. Environ. Qual.*, 9, 251-256.

Rolston, D. E., (1986) Gas flux. In *Methods of Soil Analysis, Part 1. Physical and Mineralogical Methods*. 2nd ed., Klute, A., Ed., pp 1103-1119. American Society of Agronomy, Madison, WI.

Sanders, P. F., McChesney, M.M., and Seiber, J.N., (1985) Measuring pesticide volatilization from small surface areas in the field. *Bull. Environ. Contam. Toxicol.*, 35, 569-575.

Sebacher, D. I., R. C. Harris, and K. B. Bartlett, (1983) Methane flux across the air-water interface: air velocity effects. *Tellus*, 35B, 103-109.

Weast, R. C., (1986) Handbook of Chemistry and Physics, 67th ed., CRC Press, Cleveland, OH.

Wesely, M. L., Lenschow, D. H., Denmead, O. T., (1989) Flux measurement techniques. In Global tropospheric chemistry: chemical fluxes in the *global atmosphere*. Lenschow, D. H., and Jicks, B. B., eds., pp 31-46. National Center for Atmospheric Research, Boulder, CO.

Woodrow, J. E., and Seiber, J. N., (1991) Two chamber methods for the determination of pesticide flux from contaminated soil and water. *Chemosphere*, 23, 291-304.

Yagi, K., Williams, J., Wang, N.-Y., and Cicerone, R. J., (1995) Atmospheric methyl bromide ( $\text{CH}_3\text{Br}$ ) from agricultural soil fumigation. *Science*, 267, 1979-1981.

Yates, S. R., Gan, J., Ernst, F. F., and Wang, D., (1996) Methyl bromide emissions from a covered field: III. Correcting chamber flux for temperature. *J. Environ. Qual.*, 25, 892-898.

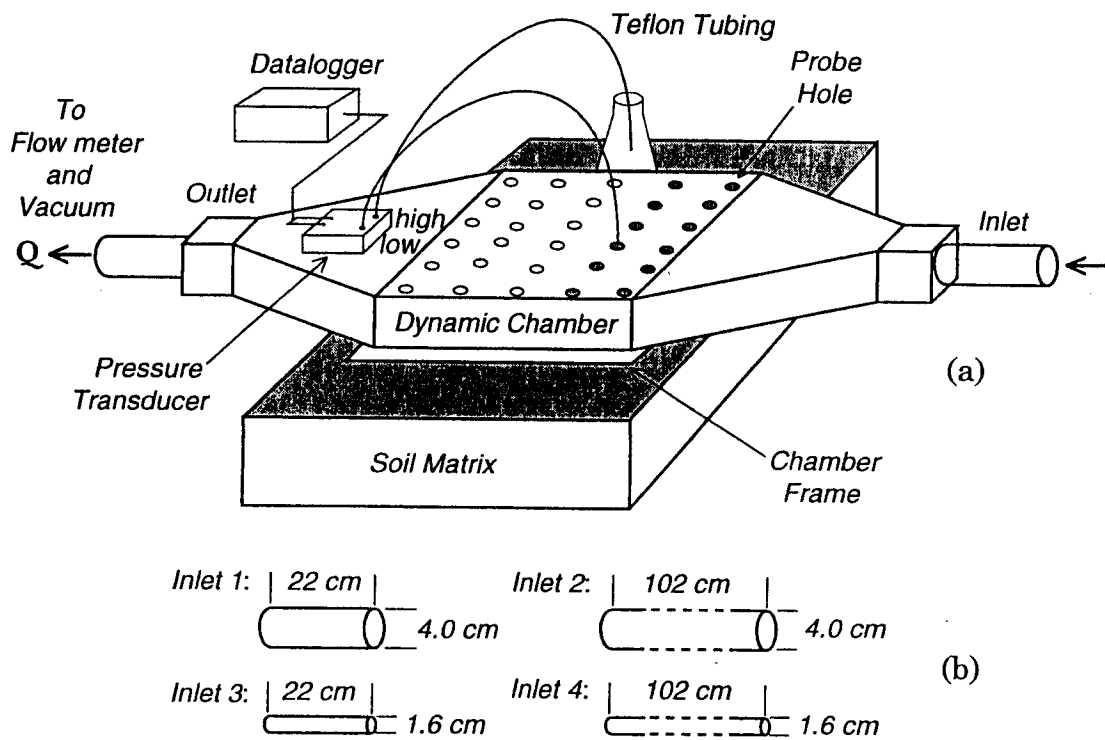


Figure 1. Experimental Setup. (a) Dynamic chamber and soil matrix. (b) Four inlets tested.

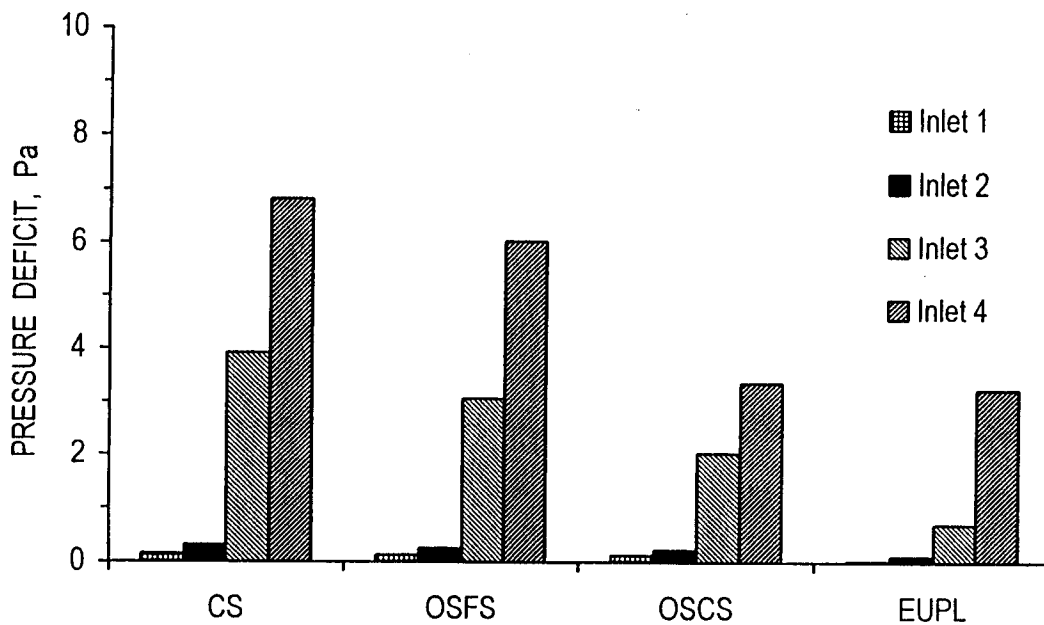


Figure 2. Measured and estimated pressure deficits within the dynamic chamber at an air flow rate of  $21 \text{ L min}^{-1}$ . CS: covered surface; OSFS: open surface of fine sands; OSCS: open surface of coarse sands; EUPL: estimated using Poiseuille's law.

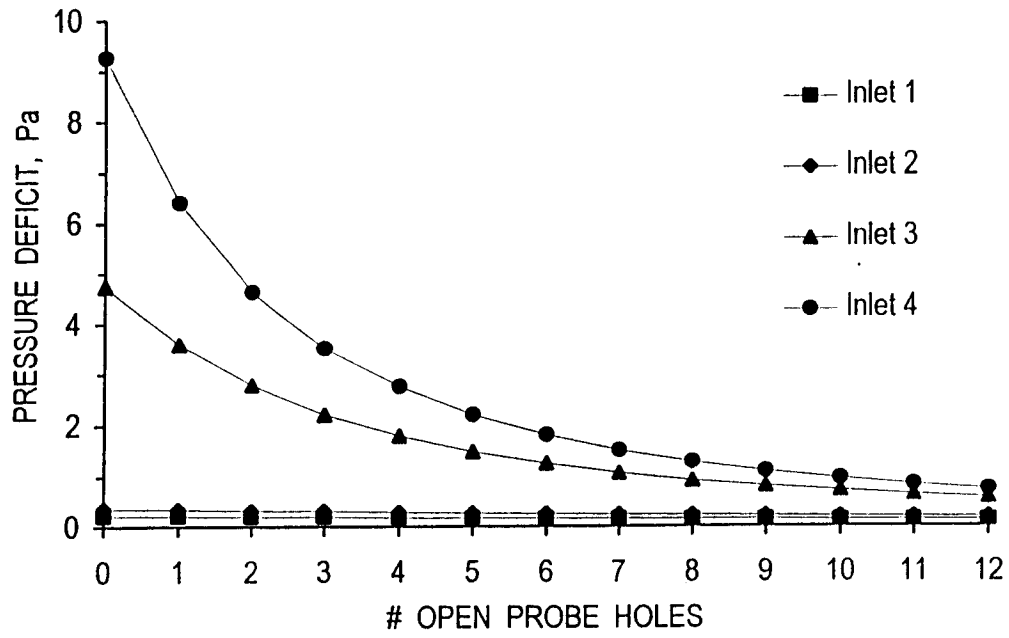


Figure 3. Pressure deficit within the dynamic chamber on fine sands at  $Q = 37 \text{ L min}^{-1}$ .

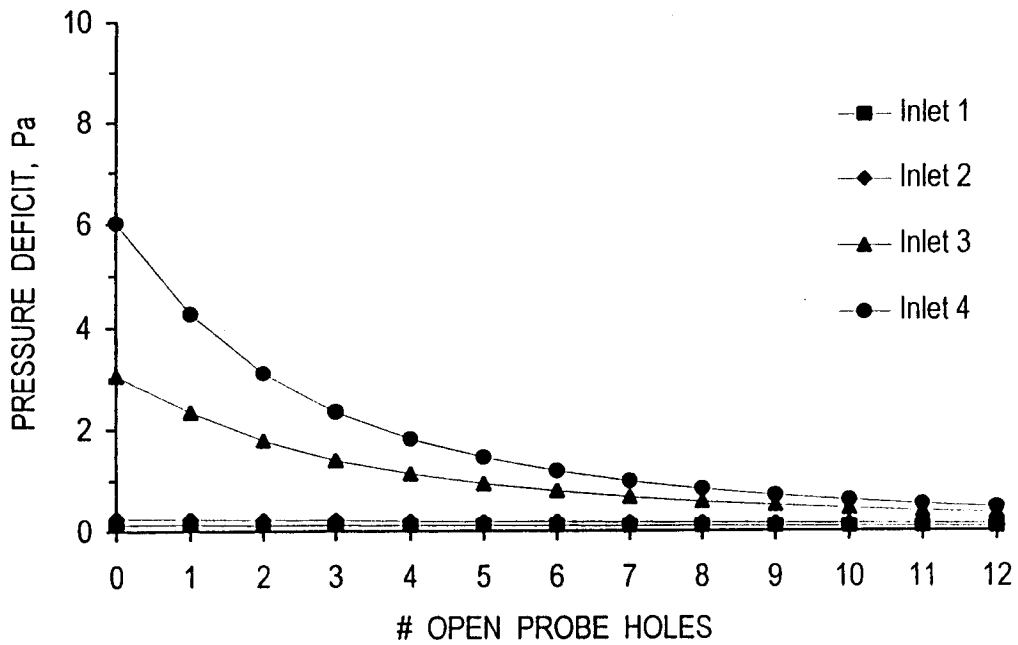


Figure 4. Pressure deficits within the dynamic chamber on fine sands at  $Q = 21 \text{ L min}^{-1}$ .

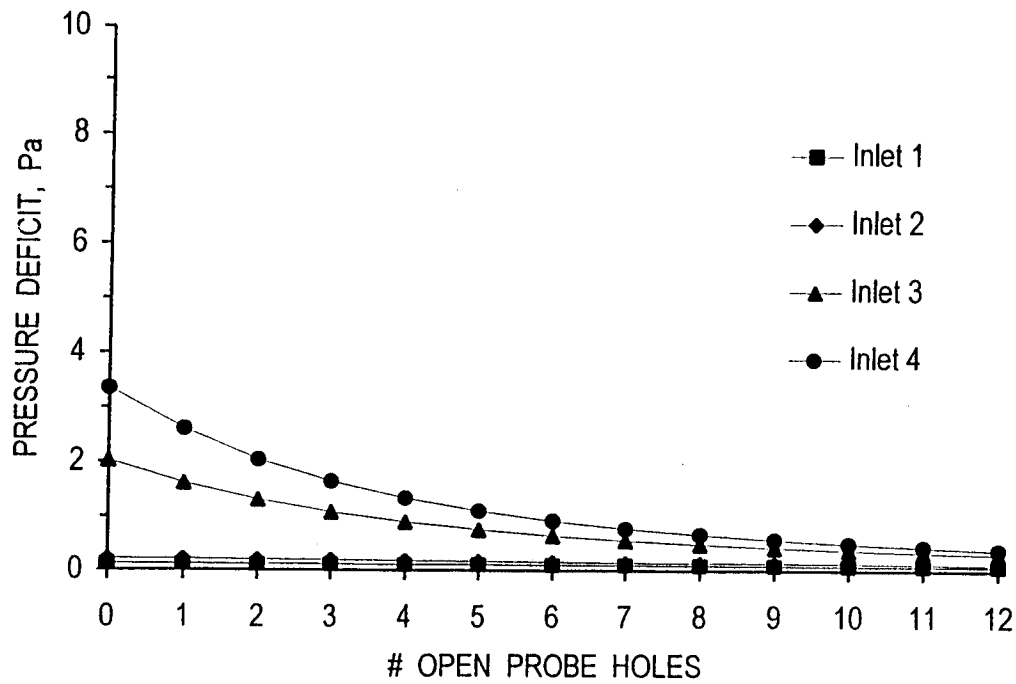


Figure 5. Pressure deficits within the dynamic chamber on coarse sands at  $Q = 21 \text{ L min}^{-1}$ .

**Table 1. Magnitudes and comparison of the pressure deficits measured in the experiment.**

Test	Chamber Inlet *	Flow rate $\text{L min}^{-1}$	Pressure deficit, Pa			
			$\Delta P_0^{**}$	$\Delta P_{12}^{**}$	$\Delta P_0 - \Delta P_{12}$	$\Delta P_{12} / \Delta P_0$
On fine sands	1	37	0.22	0.13	0.09	0.58
	2	37	0.37	0.19	0.18	0.52
	3	37	4.75	0.57	4.18	0.12
	4	37	9.26	0.74	8.52	0.08
On fine sands	1	21	0.13	0.08	0.05	0.63
	2	21	0.26	0.14	0.12	0.54
	3	21	3.05	0.36	2.69	0.12
	4	21	6.02	0.47	5.54	0.08
On coarse sands	1	21	0.12	0.08	0.04	0.67
	2	21	0.22	0.12	0.10	0.53
	3	21	2.02	0.31	1.71	0.15
	4	21	3.35	0.39	2.96	0.12

\* Inlets as indicated in Figure 1b. \*\*  $\Delta P_0$ , measured with no additional open hole;  $\Delta P_{12}$ , with 12 open holes.